Fracture properties of cement paste and mortar: an experimental investigation

Y. Zhu & S.L. Xu

Department of Civil Engineering, Dalian University of Technology, Dalian, China

ABSTRACT: Three-point bending beams of cement paste and mortar with different sizes and strengths were tested. A complete load versus crack mouth opening displacement (*P-CMOD*) curve was directly obtained, and double-*K* fracture parameters could subsequently be determined. An apparent stable crack propagation preceding unstable failure was observed in cement paste, but this stable stage shortens with the increases in the compressive strength and the size lessening, furthermore the influence of specimen size on the stage was more obvious than that of strength. The experimental results show that resistance to crack propagation in matrix is enhanced due to aggregate in the matrix, though the grain size used was very small. The double-*K* fracture parameters K_{Ic}^{ini} and K_{Ic}^{un} of cement paste are size-independent. For cement paste and mortar, due to the influence of shrinkage crack, the divergence of the unstable fracture toughness K_{Ic}^{un} is more evident than initial fracture toughness K_{Ic}^{ini}.

1 INTRODUCTION

Since fracture mechanics was applied to concrete materials in 1961 (Kaplan 1961), large quantities of experiments have been carried out to understand the fracture properties of concrete, and crack propagation in concrete (Xu 1991, Mindess 1983, 1986). Various fracture models like the fictitious crack model (Hillerborg et al. 1976), the crack band model (Bazant & Oh 1983), the two-parameter model (Jenq & Shah 1985), the size effect model (Bazant & Kazemi 1990), the effect crack model (Swartz & Go 1984, Swartz & Refai 1987, Karihaloo & Nallathambi 1989, 1990) and the double-*K* fracture criterion (Xu & Reinhardt 1998, 1999, 2000) were proposed in the last 20 years. The double-*K* fracture criterion can be used to predict crack initiation, steady crack propagation and unstable fracture. Regarding practical experimental performance in the determination of fracture parameters introduced in the double-*K* criterion, one needs to measure the ascending branch of a *P-CMOD* curve, without steady unloading procedure. It means that when a material and structural laboratory even does not have a closed-loop testing system, it can also perform the experimental measurements of the double-*K* fracture parameters K_{Ic}^{ini} and K_{Ic}^{un}. Considering the calculation of the fracture parameters, no statistical regression is necessary in the calculating procedure of the determination of the double-*K* fracture parameters K_{Ic}^{ini} and K_{Ic}^{un}. However, the studies on the double-*K* fracture criterion limit to concrete material.

As cement-based composite, concrete can be properly represented by three phases in microstructure: cement paste, aggregate as well as interfacial transition zone between them. In order to well understand crack propagation in concrete material, some authors had made many researchs on the effect of inclusions on fracture properties of concrete, such as the aggregate content (Amparano et al. 2000), the type of coarse aggregates (Hassanzadeh 1998), the mortar-aggregate interface (Lee & An 1998), the coarse/fine aggregate ratio (Zhang et al. 2004) and so on. As the matrix compositions of concrete, fracture properties of cement paste and mortar have great influence on fracture performance of concrete. It is necessary to study the basic fracture behaviors of cement paste and mortar. To gain this aim, three-point bending beams of cement paste and mortar with different sizes and strengths were tested. A complete load versus crack mouth opening displacement (*P-CMOD*) curve was directly obtained, and the double-*K* fracture parameters could subsequently be determined.

2 EXPERIMENTAL PROCEDURES

2.1 *Constituent materials*

P.O.32.5R ordinary Portland cement supplied locally conformed to China national standard GB175-92,

high-quality silica sand that the maximum size was 1.2 mm and water were used for casting cement paste and mortar specimens. Methyl cellulose (MC) was used to improve the consistency and water retentivity of cement paste, and the maximum content was 0.5%.

2.2 Casting of test specimens

To evaluate the fracture behaviors of cement paste and mortar, three-point bending beam specimens with different sizes and strengths were used (see Fig. 1). The ratio of the span to the depth of the beam (S/D) was 4 for all the specimens. The ratio of the notch length to the beam depth (a_0/D) was 0.4 for all the specimens. The thickness of all beams was equal to the beam depth. In this way, all the beams were geometrically similar in the three dimensions.

Three different beam sizes were tested. The size of the beam specimens is shown in Table 1. To examine the effect of compressive strength, three different strengths were used (see Table 1). For cement paste and mortar specimens, three strengths of beams were tested for each size except the beams of series B, and six specimens for each size, and thus, totally 84 beams were tested. Each group was ensured at least three specimens were successful. The water-cement ratios (W/C) and the MC content are also given in Table 1.

For the casting of cement paste and mortar specimens, steel moulds were used. At the same time, six 70.7×70.7×70.7 mm cubes were cast for the test of 28 days compressive strength under the same conditions as the other beam specimens. All the samples were demoulded after 48 h and cured in a fog room for 28 days. The details of the cast specimens of different categories are listed in Table 1.

2.3 Tests on specimens

The three-point bending beam tests were performed on a closed-loop, servo-hydraulic testing machine under displacement control. The rate of displacement was kept as 0.05 mm/min for the beams of series C, and 0.02 mm/min for the beams of series A and B. To measure CMOD a pair of knife edges is
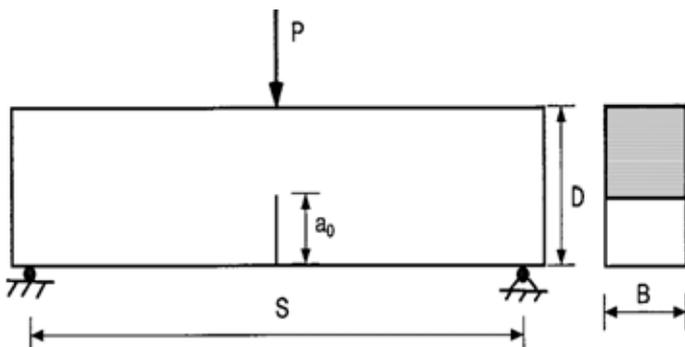
Table 1. Details of specimens

Series	Category designation	Dimensions mm	W/C	MC content %	compressive strength MPa
A	P20A	40×40×160	0.55	0.5	23.57
	P40A	40×40×160	0.45	0.4	42.77
	P60A	40×40×160	0.40		70.17
	M20A	40×40×160	0.70		33.76
	M40A	40×40×160	0.65		47.75
	M60A	40×40×160	0.40		70.07
B	P40B	70×70×280	0.45	0.4	42.77
	M40B	70×70×280	0.65		47.75
C	P20C	100×100×400	0.55	0.5	23.57
	P40C	100×100×400	0.45	0.4	42.77
	P60C	100×100×400	0.40		70.17
	M20C	100×100×400	0.70		33.76
	M40C	100×100×400	0.65		47.75
	M60C	100×100×400	0.40		70.07

attached at the two sides of a performed notch on the lower surface of the beam. The process of crack initiation, stable extension and unstable failure were investigated using resistant strain gauges that were pasted at the centre of the specimens (see Fig. 2).

3 TEST RESULTS AND ANALYSES

3.1 Determination of the initial cracking load

From the load-strain (P-ε) curve, one can see that the initial part of the curve is almost linear and the strain of the tip of the notch which is tension strain can be increased with load growing. After a linear portion of the P-ε curve, the deviation from the linear curve is observed and the tension strain reaches the maximum value, which means the onset of crack initiation at the tip of the notch. After the point of the maximum tension strain, the curve exhibits rise of load until reaches the peak and decline of tension strain even changes to compression strain.
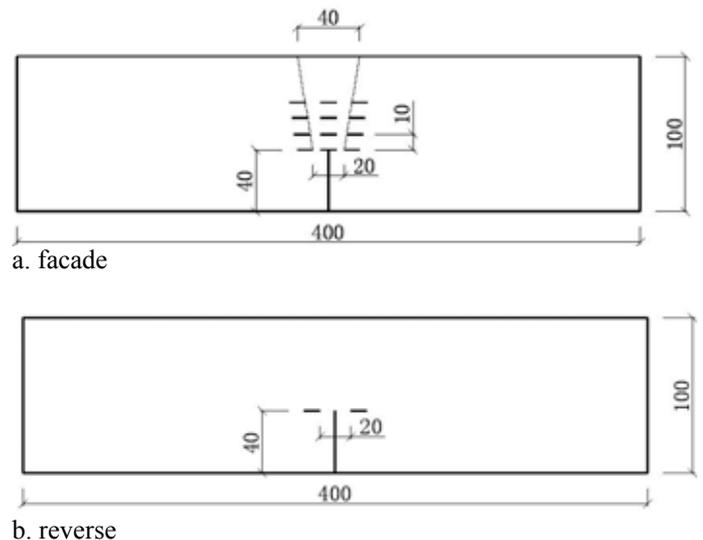

a. facade

b. reverse

Figure 2. Arrangement diagram of the strain gauges

Figure 1.Configuration of a three-point bending notched beam

Therefore, the load that the tension strain reaches its maximum value is the initial cracking load (see Fig. 3). Because the two sides of specimen can't crack at the same time, the average of load that tension strain on both the specimen sides come to peak is considered to be the initial cracking load.
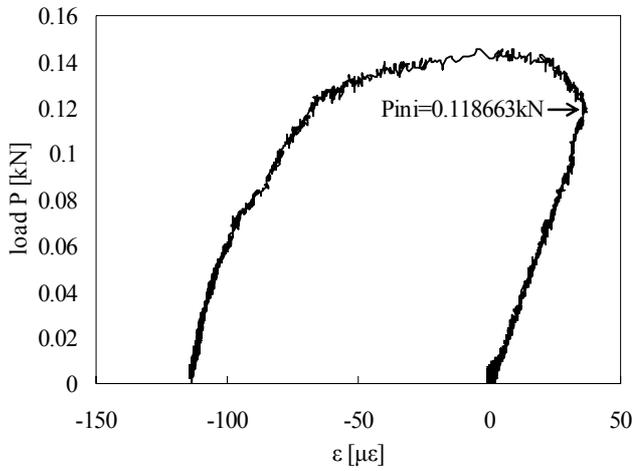

Figure 3. Determination of the initial cracking load

3.2 P-CMOD curves

Typical *P-CMOD* curves, obtained from the test, are shown in Fig. 4. All the *P-CMOD* curves of cement paste and mortar show the same pattern as concrete, which consists of three parts: (1) the linear elastic stage before crack initiation; (2) elastic-plastic stage of stable crack propagation preceding unstable failure; (3) unstable extension stage after the peak load. Although similar curve pattern between cement paste and mortar, the ultimate flexural strength of mortar is higher than that of cement paste for the same compressive strength. After specimen cracked, the load of cement paste is lower than that of mortar for the same crack width. From these phenomena, one can see that mortar have better fracture properties than cement paste for similar compressive strength, because resistance to crack propagation in
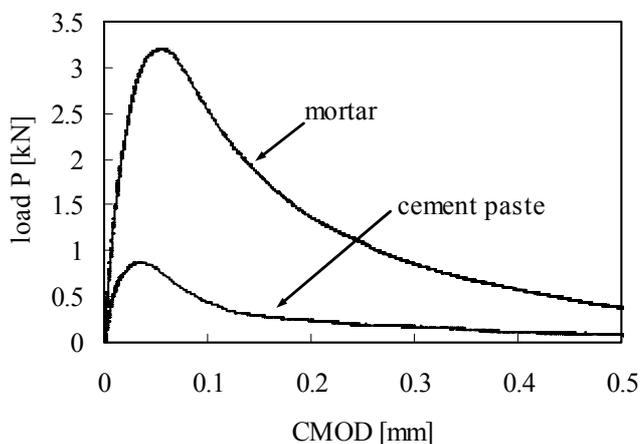

Figure 4. P-CMOD curves of different materials

matrix is enhanced due to aggregate in the matrix, though the grain size used was very small.

Fig. 5 is *P-CMOD* curves for cement paste and mortar beams of series A and C with different strengths. In the figure, the peak of *P-CMOD* curves is higher and the area under the curve is larger with strength increasing, which means that the ultimate load and fracture energy of cement paste and mortar increase when strength become higher. Therefore, their resistance to crack propagation is enhanced by increasing compressive strength. But the descending branch after peak load of *P-CMOD* curves of cement paste become steeper and their crack mouth opening displacement become smaller when strength increase, which indicates that with the increases in the compressive strength the brittleness of cement paste becomes more obvious, and it's unfavorable to the fracture properties of cement paste. For the same size specimens, the ultimate load of cement paste about strength of series 60 less than that of mortar about strength of series 20. So fracture properties of the matrix can't be improved by only increasing compressive strength.

For the same compressive strength, the influence of specimen size on *P-CMOD* curves of cement paste and mortar beams is more obvious (see Fig.6), and the bigger of specimen size the larger of area under the curve. For the same crack mouth opening displacement, the bearing capacity of large size specimen is higher. From Fig. 5 and Fig.6, one can find that the influence of specimen size on fracture properties of cement paste and mortar is more obvious than that of strength.
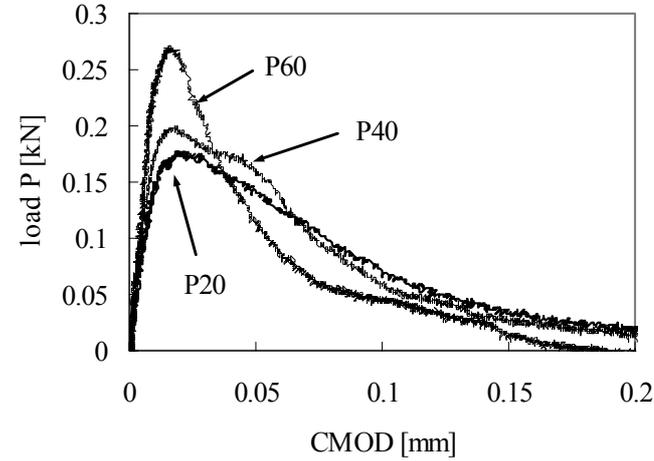
3.3 The ratio of the initial cracking load to the maximum load

The initial cracking load (P_{ini}) are given according to the above method, and the corresponding maximum load (P_{max}) are measured. Their average test results are listed in Table 2.
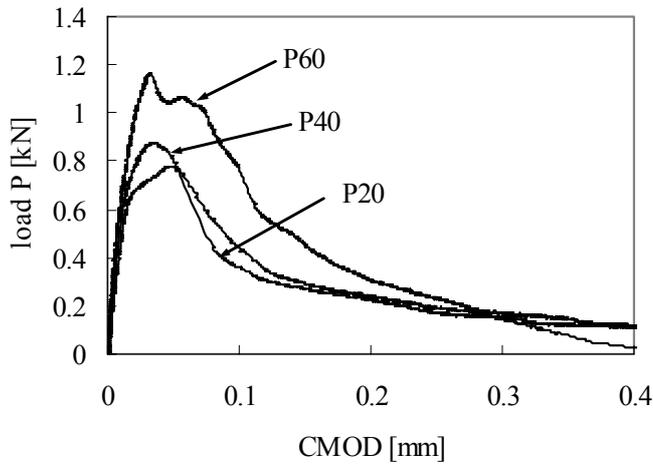
For stable crack propagation stage preceding unstable failure, namely subcritical crack growth, many people don't think this stage can be found in cement paste. They think as a brittle material, sudden brittle fracture will occurred in cement paste and the crack in it begins to expend unstably once initiation. But an apparent stable crack propagation preceding unstable failure could be observed by naked eye in cement paste, and that also can be found from the ratio of the initial cracking load to the maximum load. The increase of subcritical crack growth can cause the ratio become small. By and large, the ratios of P_{ini} to P_{max} exhibit an upward tendency with strength increasing. The possible explanation for the present result is the brittleness of cement paste and mortar become more obvious due to the increased strength, that shorten the stage of subcritical crack growth. The results are coincident with the above
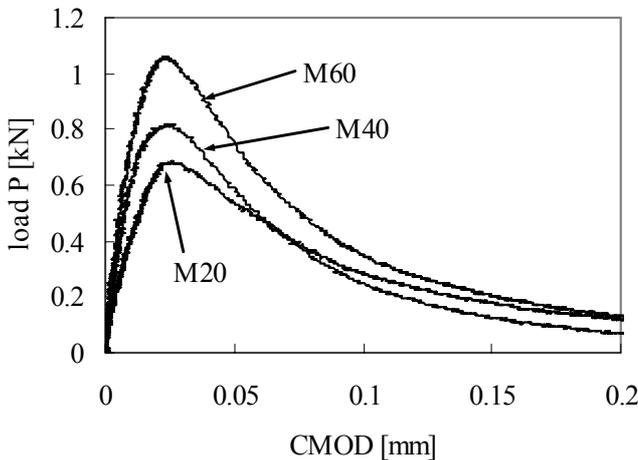
conclusions are investigated from the *P-CMOD* curves.

The influence of specimen size on the ratio of P_{ini} to P_{max} is observed in Table 2. When the respective compressive strengths of cement paste and mortar are identical, the values of P_{ini} / P_{max} are smaller for the large size specimens. Therefore, crack initiation in large size specimen is much earlier, and the stage of subcritical crack growth is much longer. The characteristic of cement paste and mortar are similar with that of concrete (Wu et al. 2001).
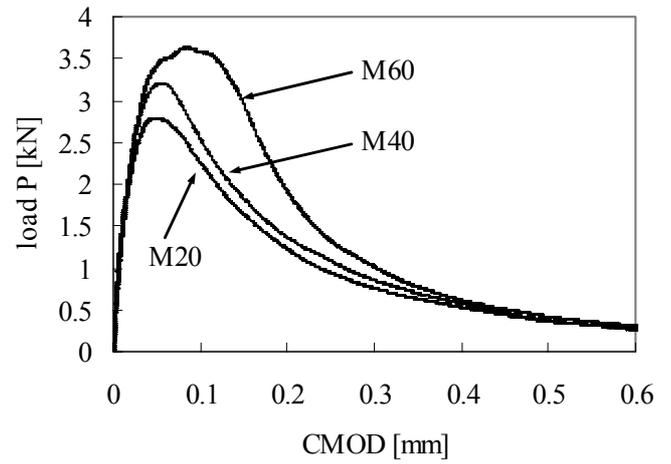
a. cement paste of series A
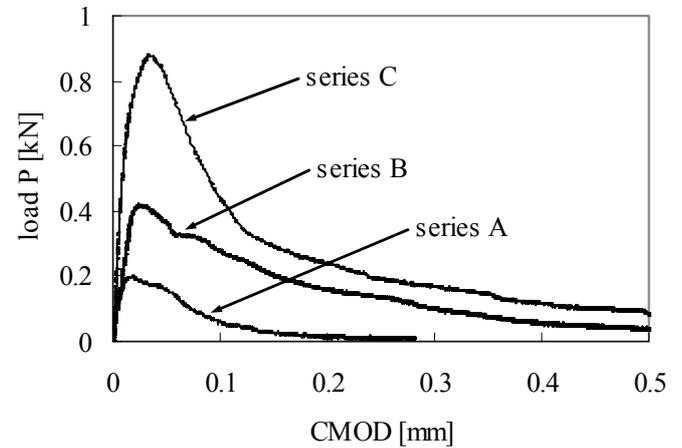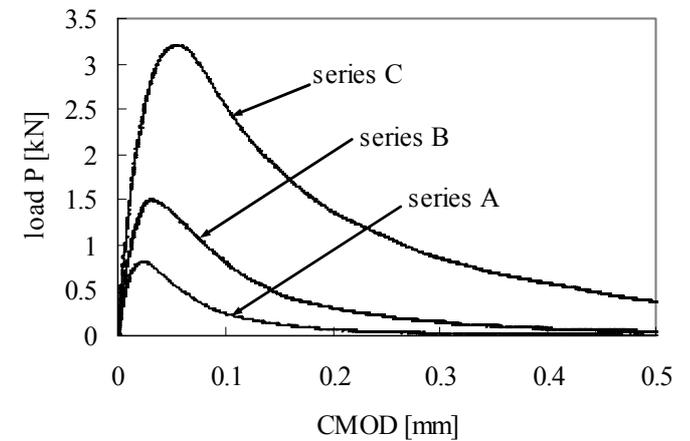
b. cement paste of series C

c. mortar of series A

d. mortar of series C

Figure 5. P-CMOD curves for cement paste and mortar with different strengths

a. cement paste

b. mortar

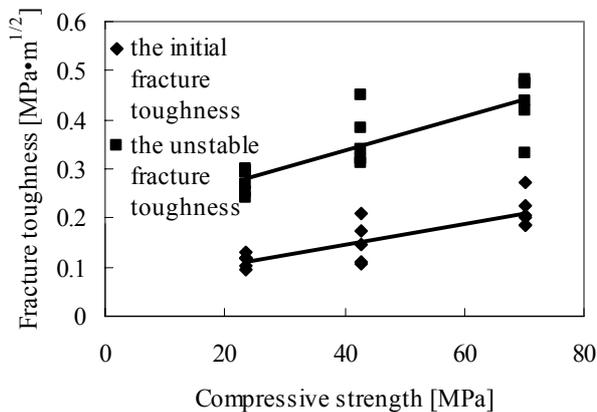Figure 6. P-CMOD curves for cement paste and mortar with different sizes

Table 2. Average test results of the initial cracking load and the maximum load

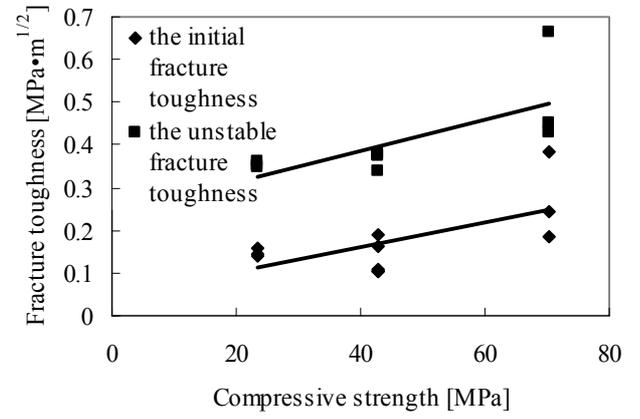| Series	Category designation	P_{ini} kN	P_{max} kN	P_{ini}/P_{max}
A	P20A	0.131777	0.192031	0.686225
	P40A	0.172019	0.224898	0.764877
	P60A	0.211557	0.269026	0.786379
	M20A	0.662718	0.708101	0.93591
	M40A	0.761317	0.893721	0.851851
	M60A	0.774889	0.968867	0.799789
B	P40B	0.448782	0.606758	0.739638
	M40B	1.235371	1.545237	0.79947
C	P20C	0.4726	0.90721	0.520937
	P40C	0.588494	0.833908	0.705706
	P60C	0.829003	1.013326	0.818101
	M20C	2.094759	2.840591	0.737438
	M40C	2.146805	2.852361	0.752641
	M60C	2.913031	3.706808	0.78586

3.4 *The double-K fracture parameters*

By using the standard three-point bending beam specimens, the unstable fracture toughness K_{Ic}^{un} of cement paste and mortar were evaluated from the maximum load P_{max} and the corresponding critical crack mouth opening displacement $CMOD_c$ was measured in experiments. The measured values of the initial fracture toughness K_{Ic}^{ini} were obtained according to the initial cracking load that determined by means of resistance strain gauge. Influence of compressive strength and specimen depth on fracture toughness of cement paste and mortar are showed in Fig.7, 8, respectively.
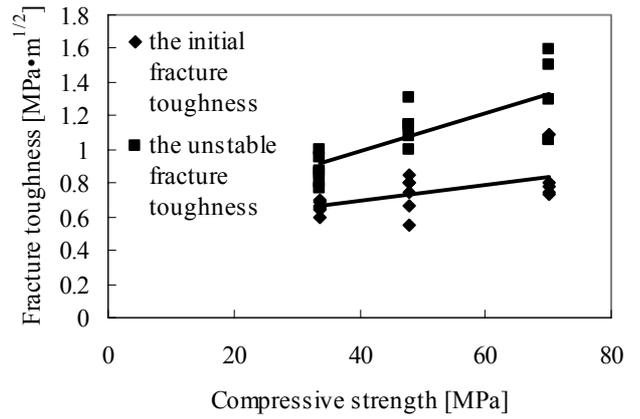
For the sizes of series A and C, although the dispersion exist in the same group of specimens, both the initial fracture toughness K_{Ic}^{ini} and unstable fracture toughness K_{Ic}^{un} obtained from cement paste and mortar specimens of same size are increased with the improvement of compressive strength, and the more improvement in compressive strength the greater increase of the double-*K* fracture parameters K_{Ic}^{ini} and K_{Ic}^{un}. Through the comparison of fracture toughness between cement paste and mortar, one can see that the aggregate in matrix is very helpful for increasing the fracture toughness of the matrix.
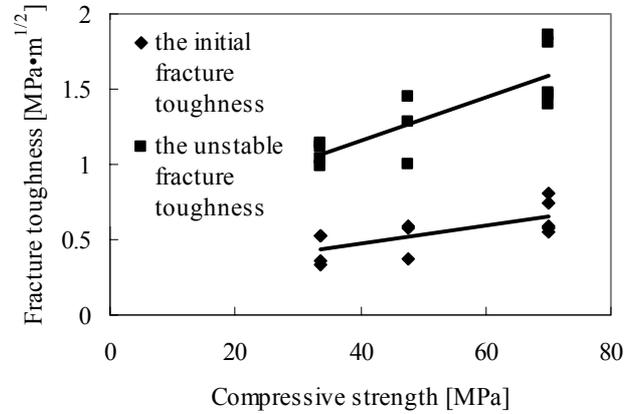

a. cement paste of series A

b. cement paste of series C

c. mortar of series A

d. mortar of series C

Figure 7. Influence of compressive strength on fracture toughness of cement paste and mortar

From Fig. 6, we have known that with increasing size of cement paste specimens, the failure load and the energy absorbed during the whole fracture process increased. But for cement paste, the double-*K* fracture parameters K_{Ic}^{ini} and K_{Ic}^{un} are almost constant with the variation of specimen size (see Fig. 8). This result indicate that the double-K fracture parameters K_{Ic}^{ini} and K_{Ic}^{un} of cement paste are size-independent. From the difference between K_{Ic}^{ini} and K_{Ic}^{un}, we also can find there is a crack propagation stage before unstable fracture in cement paste and mortar. Fur-

thermore, the divergence of the unstable fracture toughness K_{Ic}^{un} is more evident than initial fracture toughness K_{Ic}^{ini}, especially cement paste. One of the possible explanations is that there is no aggregate or small size of aggregate in them, and thus the influence of shrinkage crack is more obvious in cement paste and mortar.
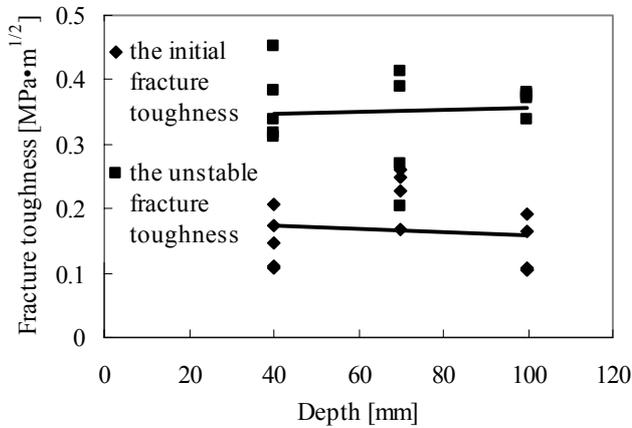

Figure 8. Influence of specimen depth on fracture toughness of cement paste

4 CONCLUSIONS

The fracture properties of cement paste and mortar with different sizes and strengths were tested by 84 geometrically similar three-point bending beams of cement paste and mortar, and their double-K fracture parameters were given subsequently. Fracture properties of cement paste and mortar depend strongly on both specimen size and strength. When strength become higher, the ultimate load, fracture toughness and fracture energy of cement paste and mortar increase. But for cement paste, the post-peak (after maximum loads) section of the *P-CMOD* curves exhibit much more steeper and the critical crack mouth opening displacement becomes smaller with the increases in the compressive strength, which can be explained by the brittleness of cement paste becomes more obvious when compressive strength increase, and it's unfavorable to the fracture properties of cement paste. It also can be find that fracture properties of the matrix can't be improved by only increasing compressive strength and the aggregate in matrix, though the grain size used was very small, is very helpful for improving fracture properties of the matrix.

An apparent stable crack propagation preceding unstable failure could be observed in cement paste by naked eye in the test, and that also can be found from the ratio of the initial cracking load to the maximum load and the difference between the initial fracture toughness K_{Ic}^{ini} and the unstable fracture toughness K_{Ic}^{un}. But this stable stage shortens with the increases in the compressive strength and the

size lessening, furthermore the influence of specimen size on the stage is more obvious than that of compressive strength.

For cement paste and mortar, the influence of shrinkage crack is obvious because of no aggregate or small size of aggregate therefore the divergence of the unstable fracture toughness K_{Ic}^{un} is more evident than initial fracture toughness K_{Ic}^{ini}, especially cement paste. And the double-K fracture parameters K_{Ic}^{ini} and K_{Ic}^{un} of cement paste are size-independent.

ACKNOWLEDGEMENT

REFERENCE

Amparano, F.E., Xi, Y.P., Roh, Y.S. 2000. Experimental study on the effect of aggregate content on fracture behavior of concrete. *Engineering Fracture Mechanics* 67(1):65-84.

Bazant, Z.P. & Oh, B.H. 1983. Crack band theory for fracture of concrete. RILEM. *Materials and Structures* 16(93): 155-177.

Bazant, Z.P. & Kazemi, M.T. 1990. Determination of fracture energy, process zone length and brittleness number from size effect, with application to rock and concrete. *International Joural of Fracture* 44: 111-131.

Hassanzadeh, M. 1998. The influence of the type of coarse aggregates on the fracture mechanical properties of high performance concrete. In: Mihashi, H. and Rokugo, K., editors, Fracture Mechanics of Concrete Structures, Proc. of FRAMCOS-3. D-79104 Freiburg: Aedificatio Publishers, pp: 161-170.

Hillerborg, A., Modeer, M., Petersson, P.E. 1976. Analysis of crack formation and crack growth in concrete by means of fracture mechanics and finite elements. *Cement and Concrete Research* 6: 773-782.

Jenq, Y.S. & Shah, S.P. 1985. A fracture toughness criterion for concrete. *Engineering Fracture Mechanics* 21(5): 1055-1069.

Jenq, Y.S. & Shah, S.P. 1985. Two parameter fracture model for concrete. *Journal of Engineering Mechanics* 111(10): 1227-1241.

Kaplan, M.F. 1961. Crack propagation and the fracture of concrete. *Journal of American Concrete Institute* 58(5):591-610.

Karihaloo, B.L. & Nallathambi, P. 1989. An improved effective crack model for the determination of fracture toughness of concrete. *Cement and Concrete Research* 19: 603-610.

Karihaloo, B.L. & Nallathambi, P. 1990. Effective crack model for the determination of fracture toughness (K_{Ic}^{s}) of concrete. *Engineering Fracture Mechanics* 35(4/5): 637-645.

Lee, K.M. & An, K.S. 1998. Factors influencing fracture toughness of mortar-aggregate interface in concrete. In: Mihashi, H. and Rokugo, K., editors, Fracture Mechanics of Concrete Structures, Proc. of FRAMCOS-3. D-79104 Freiburg: Aedificatio Publishers, pp: 193-202.

Mindess, S. 1983. The cracking and fracture of concrete: an annotated bibliography 1928-1981. Fracture Mechanics of Concrete (edited by Wittmann F H). Elsevier Science Publishers B. V., The Netherlands, pp: 539-661.

Mindess, S. 1986. The cracking and fracture of concrete: an annotated bibliography 1982-1985. Fracture Toughness and Fracture Energy of Concrete (edited by Wittmann F H). Elsevier Science Publishers B. V., The Netherlands, pp: 629-694.

Swartz, S.E. & Go, C.G. 1984. Validity of compliance calibration to cracked concrete beams in bending. *Experimental Mechanics* 24(2): 129-134.

Swartz, S.E. & Refai, T.M.E. 1987. Influence of size on opening mode fracture parameters for precracked concrete beams in bending. Proceedings of SEM-RILEM International Conference on Fracture of Concrete and Rock (Edited by S.P. Shah and S.E. Swartz), Houston, Texas, pp: 242-254.

Wu, Z.M., Xu, S.L., Liu, J.Y. 2001. Study on crack propagation process of concrete and size effect of double-*K* fracture parameters by means of photoelastic coatings. *Journal of Hydraulic Engineering* 4: 34-39.

Xu, S.L. & Zhao, G.F. 1991. Study on fracture mechanics of concrete. Dalian: Press of Dalian University of Technology.

Xu, S.L. & Reinhardt, H.W. 1998. Determination of double-*K* fracture parameters in standard three-point bending notched beams. Fracture Mechanics of Concrete Structures, Proc. of FRAMCOS-3 (Edited by Mihashi, H. and Rokugo, K.), Aedificatio Publishers, Freiburg, Germany 1: 431-440.

Xu, S.L. & Reinhardt, H.W. 1999. Determination of double-*K* criterion for crack propagation in quasi-brittle materials, part : analytical evaluating and practical measuring methods for three-point bending notched beams. *International Journal of Fracture* 98(2): 151~177.

Xu, S.L. & Reinhardt, H.W. 2000. A simplified method for determining double-K fracture parameters for three-point bending tests. *International Journal of Fracture* 104: 181-209.

Zhang, J., Wang, L., Sun, M., Liu, Q. 2004. Effect of coarse/fine aggregate ratio and cement matrix strength on fracture parameters of concrete. *Engineering Mechanics* 21(1): 136-142.